Influence of Temperature Variation on Optical Receiver Sensitivity and its Compensation

Aleš PROKEŠ

Dept. of Radio Electronics, Brno University of Technology, Purkyňova 118, 612 00 Brno, Czech Republic

prokes@feec.vutbr.cz

Abstract. *In the paper, the influence of temperature variation on the sensitivity of an avalanche-photodiode-based optical receiver applied in the free space optical communication link is discussed. Communication systems of this type are exposed to a wide range of operating temperatures, which markedly affect many photodiode and preamplifier parameters. The paper presents a receiver sensitivity calculation, taking into consideration the temperature dependence of avalanche photodiode gain, excess noise factor, dark current and thermal noise of preamplifier resistances, and describes the compensation of temperature effects on photodiode gain based on a corresponding change in the reverse voltage applied to the diode. The calculations are demonstrated on the connection of a small-area silicon APD operating in the wavelength range from 820 to 1150 nm with a transimpedance preamplifier using a bipolar junction transistor.*

Keywords

Avalanche photodiode, photodiode gain, excess noise factor, temperature compensation, receiver sensitivity.

1. Introduction

The primary factor that determines receiver sensitivity is the amount of noise present in a photodiode and in the following preamplifier. It consists of three basic components: thermal (Johnson) noise, shot noise and 1/*f* noise. The thermal noise is present in all electronic elements containing a resistive component through which the current flows. It appears due to the random fluctuations of charge carriers inside resistor R. The single-sided power spectral-density (PSD) of thermal noise is given by [1]

$$i_t^2(f) = \frac{4kT}{R} \tag{1}$$

where k = 1.38·10-23 J/K is Boltzmann's constant, T is the absolute temperature, and R is the resistance.

The shot noise is generated by current flowing through the p-n junction. It is caused by the passage of charge carriers across the potential barrier. In the case of photodiode this current may be either the dark current (when no light is incident upon the photodiode) or the photocurrent. The normalized single-sided PSD of shot noise can be calculated by the formula

$$i_{sh}^2(f) = 2qI_{DC} \tag{2}$$

where $q = 1.6\cdot10^{-19}$ C is the charge of an electron and I_{DC} is the DC current flowing through the junction.

The 1/*f* noise is caused by the fluctuations in the resistance of a semiconductor. The normalized single-sided PSD of 1/*f* noise is given by

$$i_f^2(f) = \frac{af_c I_{DC}^m}{f^n} \tag{3}$$

where a is a constant that expresses the absolute level, m and n are numerical constants and f_c is the 1/*f* noise corner frequency. For a typical 1/*f* noise n = 1, and (3) indicates that the 1/*f* noise power is inversely proportional to the frequency. Note that for any decade in frequency the noise power is identical. The amount of 1/*f* noise at the optical receiver output strongly depends on the type of transistor used in the first stages of the amplifier. Silicon bipolar junction transistors exhibit small amounts of 1/*f* noise because their corner frequency f_c is in the region of tens of kHz. However, in the case of some GaAs field-effect transistors the corner frequency f_c can be as high as 100 MHz and the 1/*f* noise has to be considered in the receiver design.

2. Input Circuits of Optical Receiver

The input circuit of an optical receiver consists of a photodiode and a low-noise amplifier. The most frequently used amplifiers are usually grouped into two basic configurations: high-impedance (HZ) and transimpedance (TZ) amplifiers.

The high-impedance amplifier shown in Fig. 2(a) [1], [2] offers a high sensitivity since the high load impedance R_L exhibits a low noise level (1). However, the frequency response is limited by the large time constant $\tau = (C_p + C_A)R_L$, where C_p is the photodiode capacitance and C_A is the input amplifier capacitance. The ampli-

fier bandwidth is then relatively narrow. Thus to extend the receiver bandwidth to the desired value an equalizer following the amplifier is necessary. The overall amplifier transimpedance is given by the ratio of the Fourier transform of the signal voltage $V_y(f)$ to the photodiode current $I_p(f)$

$$Z_T(f)=\frac{V_y(f)}{I_p(f)}=R_L A(f)K(f) \tag{4}$$

where $A(f)$ is the amplifier open-loop voltage gain, and $K(f)$ is the equalizer transfer function.

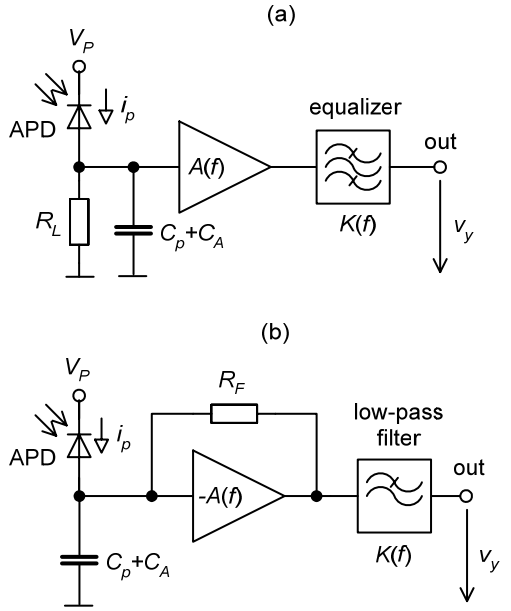

Fig. 1. Typical configurations of the receiver amplifier: High-impedance amplifier (a) and transimpedance amplifier (b).

The front-end architecture of the receiver amplifier, which provides an appropriate compromise between the low-noise and the wide-band characteristics, is of the transimpedance type. It uses a feedback resistor around the inverting amplifier as shown in Fig. 1(b). The low value of the feedback resistance R_F extends the amplifier bandwidth, but increases the thermal noise. The receiver noise bandwidth can be then reduced to the desired value by a low-pass filter following the amplifier. The overall amplifier transimpedance is

$$Z_T(f)=\frac{V_y(f)}{I_p(f)}=-R_F\frac{A(f)}{1+A(f)}K(f) \tag{5}$$

In the case of a very high amplifier open-loop gain the frequency dependence of transimpedance is determined only by the low-pass filter transfer function since $Z_T(f) = R_F K(f)$. It is obvious that wide-band and high-sensitivity receiver characteristics can be achieved by choosing a large feedback resistance and by increasing the amplifier open-loop gain.

2.1 Photodiode Equivalent Circuit

The equivalent circuit of an avalanche photodiode (APD) is shown in Fig. 2(a). It can be simplified as shown in Fig 2(b). The signal current i_{sp} and the RMS value of the noise current I_{np} can be expressed by the formulae [1]

$$i_{sp} = I_{DU} + M\left(I_{DM} + RP_r\right) \tag{6}$$

and

$$\begin{aligned} I_{np} &= \sqrt{I_{shm}^2 M^2 F(M) + I_{shu}^2} \\ &= \sqrt{2q\left(I_{DM} + R\overline{P_r}\right)\cdot M^2 F(M) I_2 R_b + 2qI_{DU} I_2 R_b} \end{aligned} \tag{7}$$

where M is the average multiplication coefficient often presented as the APD gain, P_r is the input optical power, I_{DU} is the dark current component that is not subject to the avalanche multiplication process (surface current), I_{DM} is the dark current that undergoes the multiplication process (bulk current), I_{shm} and I_{shu} are the photodiode multiplied and non-multiplied shot noises, $F(M)$ is the avalanche excess noise factor that depends on the multiplication coefficient for a given carrier ionization ratio k_i according to [3]

$$F(M) = k_i M + (1-k_i)(2-1/M), \tag{8}$$

R is the responsivity of the photodiode given by

$$R = \frac{\eta q}{hc}\lambda \tag{9}$$

where $\eta \in \langle 0.7,\ 0.8\rangle$ is the photodiode quantum efficiency, $h = 6{,}625\cdot10^{-34}$ J/s is the Planck constant and $c = 3\cdot10^{-8}$ m/s is the speed of light in a vacuum, I_2 is the weighting function, which depends on the input pulse shape and the equalized output pulse shape [2], and R_b is the operating bit-rate.

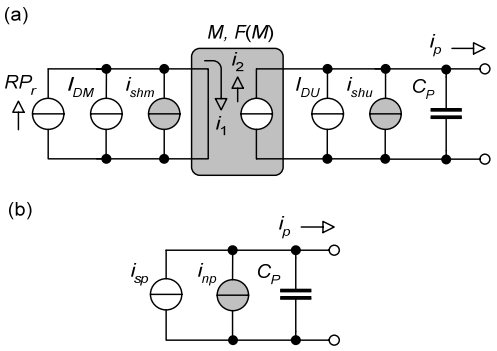

Fig. 2. APD equivalent circuit (a), simplified APD equivalent circuit (b).

The excess noise factor represents the increase in noise level during the carrier multiplication, and the product I_2R_b determines the equivalent noise bandwidth. The strongly temperature-dependent quantities are M, $F(M)$, I_{DM}, I_{DU}, and consequently I_{shm} and I_{shu}. The more detailed APD equivalent circuit also contains two resistive components junction resistance and serial resistance that exhibit thermal noise, but due to its relatively low level it can be neglected.

2.2 Amplifier Noise

The calculation of the RMS value of the input-related equivalent noise current I_{ni} is presented in many publications [1] – [4]. For the bipolar junction transistor used at the amplifier input it is given by

$$I_{ni}=\left[\frac{4kT}{R_F}I_2R_b+2q\frac{I_C}{\beta}I_2R_b+4kTr_b\left(2\pi C_P\right)^2I_3R_b^3+\frac{2qV_T^2}{I_C}\left[2\pi\left(C_T+C_P\right)\right]^2I_3R_b^3\right]^{1/2} \tag{10}$$

where R_F is the feedback resistance in the TZ design or load resistance in the HZ design, β is the current gain, I_3 is the weighting function, which depends on the input pulse shape and the equalized output pulse shape (similar to I_2) [2], r_b is the spreading base resistance of the transistor and $V_T = kT/q$ is the thermal voltage. For room-temperature operation V_T is equal to 0.0259 V. The total input capacitance is given by $C_T = C_A + C_P$, where the preamplifier capacitance C_A is composed of small-signal π-model transistor capacitances C_π and C_μ [1], and C_P includes the photodiode and stray capacitances. It can be seen that $I_{ni} = \infty$ if the collector bias current $I_C = 0$ or if $I_C = \infty$. It follows that there is an optimal value of I_C which minimizes I_{ni}. However, if the transistor operates away from its optimum bias current, the increase in the noise power relative to its optimized value is usually low.

3. Receiver Sensitivity Determination

A typical optical receiver configuration is shown in Fig. 3. The signal and noise current sources of the photodiode are discussed in chapter 2.1, and the amplifier noise current source in chapter 2.2. The decision circuit (DC) connected at the amplifier output compares the amplifier output voltage v_y with the threshold voltage V_T. For the purpose of sensitivity calculation the Gaussian probability density distribution of the amplifier output noise is assumed. The overall transimpedance $Z_T(f)$ is assumed to be constant and real in the frequency band R_bI_2 and the modulation used is the on-off keying (OOK).

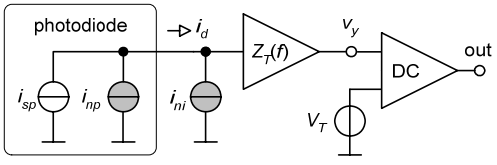

Fig. 3. Typical optical OOK receiver configuration.

The receiver sensitivity is defined as the minimum received optical power that causes symbol detection with a given bit error probability $P_{e0,1}$. It can be expressed in the form [1]

$$P_{e0,1}=P(0)\Phi\left(\frac{V_T-V_0}{\sigma_0}\right)+P(1)\Phi\left(\frac{V_1-V_T}{\sigma_1}\right) \tag{11}$$

where $\Phi(.)$ is the normalized probability distribution function, $P(1)$ and $P(0)$ are the probabilities of symbol occurrence,

$$V_i=Z_T\left[I_{DU}+M\left(I_{DM}+RP_{ri}\right)\right],\quad i=0,1 \tag{12}$$

is the symbol voltage,

$$\sigma_i=Z_T\left[2q\left(RP_{ri}+I_{DM}\right)M^2F\left(M\right)I_2R_b+2qI_{DU}I_2R_b+I_{ni}^2\right]^{1/2} \tag{13}$$

is the RMS value of the noise voltage at the input of the decision circuit, and P_{ri}, (i = 0, 1) is the receiving power corresponding to the symbol 1 or 0. The probability of the occurrence of the two symbols in a data stream is usually equal and then $P(1) = P(0) = 0.5$. This equality will be assumed in the following text.

The criterion for optimum threshold setting is usually based on the assumption that the probability of mistaking the symbol 0 for the symbol 1 is equal to the probability of mistaking the symbol 1 for the symbol 0, i.e. $\left(V_T-V_1\right)/\sigma_1=\left(V_0-V_T\right)/\sigma_0$.

The threshold voltage is then given by

$$V_T=\frac{V_0\sigma_1+V_1\sigma_0}{\sigma_1+\sigma_0}. \tag{14}$$

The arguments of the above probability distribution functions define the so called Q – factor

$$Q=\frac{V_T-V_0}{\sigma_0}=\frac{V_1-V_T}{\sigma_1}. \tag{15}$$

Substituting (12), (13) and (14) into (15) and then solving (15) for P_{r1} under the simplifying conditions P_{r0} = 0 and $I_{DU} = 0$, the sensitivity can be expressed in the form

$$P_{r1}=\frac{2Q}{RM}\left[qF\left(M\right)QR_bI_2M+\sqrt{2qI_{DM}F\left(M\right)I_2R_bM^2+I_{ni}^2}\right]. \tag{16}$$

The value of the Q – factor for a given $P_{e0,1}$ can be obtained by substituting (15) into (11) and by solving the inverse probability distribution function for $P_{e0,1}$. The calculated values of the Q – factor for typical values of $P_{e0,1}$ used for optical receiver sensitivity definition are shown in Tab. 1.

$P_{e0,1}$	Q
10^{-6}	4,75
10^{-9}	6
10^{-10}	6,3
10^{-12}	7

Tab. 1. Calculated Q – factor for typical bit error probabilities.

It can be seen that the sensitivities of an optical receiver for two different values of $P_{e0,1}$ e.g. $P_{e0,1} = 10^{-12}$ and $P_{e0,1} = 10^{-9}$ are in the ratio of 7/6 (0.67 dB).

4. Dependence of APD Parameters on Temperature

An example of the dependence of APD total responsivity

$$R_T = MR \tag{17}$$

on the reverse voltage applied to the typical small area silicon photodiode (Perkin Elmer C30902 and C30921 [4]) at specific temperatures in the range $T_A \in \langle$-40°C, 60°C$\rangle$ is given in Fig. 4.

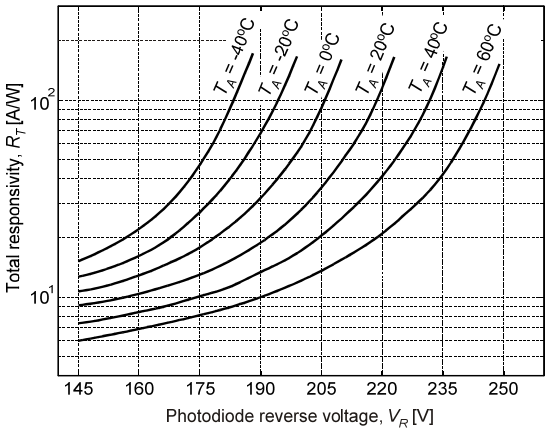

Fig. 4. Total responsivity vs. reverse voltage of photodiodes C30902 and C30921 at specific temperatures.

From the curves the magnitudes of the total responsivity at specific temperatures can be read for constant reverse voltages. Using the least squares method implemented, for example in the Matlab `polyfit` function, the above relations can be expressed with a sufficient accuracy by the fourth-order polynomials

$$R_T(T_A) = a_4 T_A^{\,4} + a_3 T_A^{\,3} + a_2 T_A^{\,2} + a_1 T_A + a_0 \tag{18}$$

where a_i, i = 0,1,..,4 are the polynomial coefficients at a specific reverse voltage. The calculated dependence of total responsivity on temperature at specific reverse voltages is shown in Fig. 5.

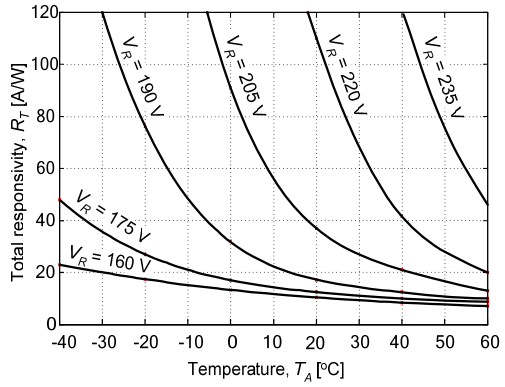

Fig. 5. Calculated dependence of total responsivity on temperature of photodiodes C30902 and C30921 at specific reverse voltages.

The values from Fig. 5 allow us to determine the temperature dependence of the excess noise factor according to (8), where we have to substitute M from (17) and R from (9). The plot of the excess noise factor vs. temperature for k_i = 0.02, λ = 830 nm, η = 0.75 [4] and reverse voltages of 190 V, 205 V and 220 V, at which the APD is usable, is shown in Fig. 6.

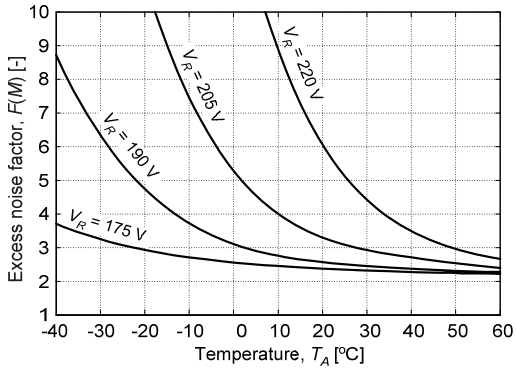

Fig. 6. Calculated dependence of excess noise factor on temperature T_A of photodiodes C30902 and C30921 at specific reverse voltages.

Note that the carrier ionization ratio in silicon is a function of the APD reverse voltage and operating temperature. It increases with the decreasing temperature. The mathematical expressions of these phenomena are difficult to find but fortunately the influence of temperature and reverse voltage on ionization ratio is not critical and can be neglected.

Another strongly temperature-dependent parameter is the dark current I_D. It is a significant contributor to the shot noise as evident from (7). The total dark current presented usually in datasheets is given by

$$I_D = I_{DU} + MI_{DM} \tag{19}$$

and the temperature dependence of its both multiplied and unmultiplied components is described by the formula [5]

$$I(T) = I_0 \exp(-qN/kT) \tag{20}$$

where N is the activation energy, and I_0 is the reverse saturation current. The activation energy is approximately 0.55 eV for the multiplied component of the dark current, while the unmultiplied component was found to have the activation energy of about 0.7 eV. The dependence of the total dark current and its components on temperature is plotted in Fig. 7. The reverse saturation current was found by solving (19) and (20) for the catalogue values $I_D \approx$ $\approx$ 1.5 nA at T = 295 K and M = 50.

Since the current I_{DM} significantly exceeds I_{DU} and its influence on the photodiode noise is considerably larger than the influence of I_{DU} due to multiplying I_{DM} by the term $M^2F(M)$, the I_{DU} can be neglected. The dark current is also affected by the photodiode reverse voltage. Its change in the voltage range from 190 V to 220 V is less than 15 % [4] and due to its difficult description will not be considered in the sensitivity calculation.

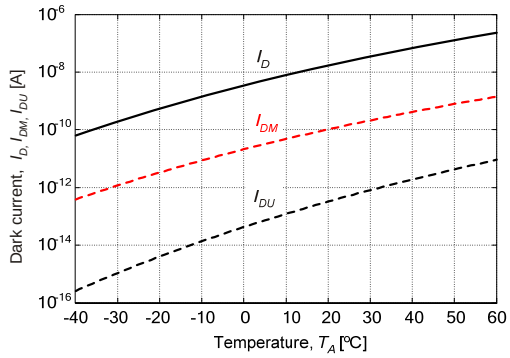

Fig. 7. Calculated dependence of dark current and its components on temperature T_A of silicon APDs C30902 and C30921.

5. Calculation of Temperature Dependence of Receiver Sensitivity

The receiver sensitivities for the data rates $R_b = 0.1$ Gbit/s and $R_b = 1$ Gbit/s are depicted in Fig. 8 and Fig. 9. The current noise related to the input I_{ni} was calculated according to (10) for the values: $I_2 = 1.05$, $I_3 = 0.52$ (NRZ coding format equalized with a third-order Butterworth filter [1]), $r_b = 20\ \Omega$, $C_P = 1.6$ pF, $C_\pi = 1.0$ pF and $C_\mu = 0.05$ pF. The feedback resistance is assumed to vary in inverse proportion to the bit-rate. The product $R_F R_b$ is thus constant and taken to be 75 kΩ·Mbits/s. The collector bias current $I_C = 0.4$ mA was chosen higher relative to its optimum value in order to avoid the drop in the current gain and cutoff frequency of the transistor.

The parameters of APD used for the sensitivity calculation are given in Fig. 4 to Fig. 7. The transimpedance is equal to R_F, i.e. $Z_T = 0.75$ kΩ for $R_b = 0.1$ Gbit/s and $Z_T = 75\ \Omega$ for $R_b = 1$ Gbit/s.

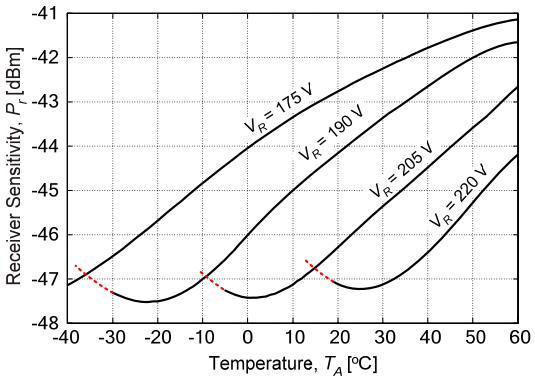

Fig. 8. Received optical power vs. temperature T_A at specific reverse voltages and at data rate $R_b = 0.1$ Gbit/s.

The sensitivity calculation was performed for the usually used value of bit error probability $P_{e0,1} = 10^{-9}$. From Tab. 1 it can then be found that $Q = 6$.

It is obvious from the figures that the receiver sensitivity decreases (the minimum input optical power increases) as the temperature increases. This is caused by the thermal noise of the preamplifier increasing and by the APD multiplication factor decreasing. It can be simply verified that a very important component of the total noise is the thermal noise generated by resistance R_F. Thus the receiver noise can be minimized by choosing a high value of R_F, but the time constant $\tau \approx R_F(C_T + C_P)$ must not limit the frequency range of the preamplifier. The influence of excess noise factor is evident at lower temperatures, where the current noise of the preamplifier is relatively low. A high excess-noise factor will result in increasing the photodiode noise and decreasing the receiver sensitivity.

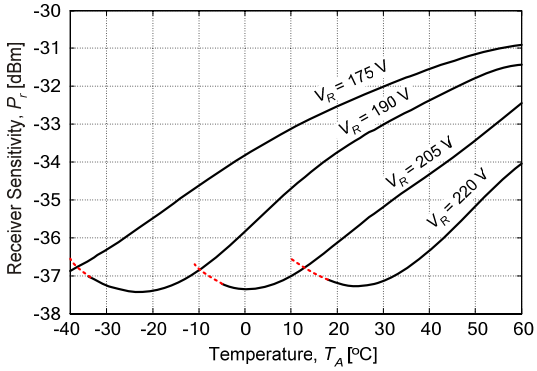

Fig. 9. Received optical power vs. temperature T_A at specific reverse voltages and at data rate $R_b = 1.0$ Gbit/s.

6. Temperature Compensation of Gain

As presented in the previous chapter, the APD total responsivity is a significant parameter that affects the receiver sensitivity. Therefore the change in responsivity caused by temperature variation is suitable to compensate. The most popular method is based on a change in the reverse voltage applied to the diode in dependence on temperature.

Similar to what was presented in Chapter 4, the magnitudes of the reverse voltages at specific temperatures can be read for constant responsivity values from the curves in Fig. 4. The relations obtained are given in Fig. 10. They can be expressed by the polynomial

$$V_R(T_A) = 0.92 \cdot 10^{-3} T_A^{\,2} + 0.60 T_A + V_R(0) \qquad (21)$$

where $V_R(0)$ is the voltage across the diode at zero temperature.

In view of the comparatively high necessary voltage V_R, the solution of power supply operating in the switched mode seems to be of advantage. The power supply of this type, using the temperature-dependent element in the feedback loop, is presented in [6]. A similar connection, using a microcontroller, is shown in Fig. 11. Power is supplied to transformer Tr at the time when transistor T is switched on. Controlling the ratio of switched-on time to switched-off time via pulse width modulation (PWM) maintains the approximate equality of voltages V_C and V'_D. The voltage V'_D read at output of analog-to-digital converter (ADC) is the quantized value of voltage V_D.

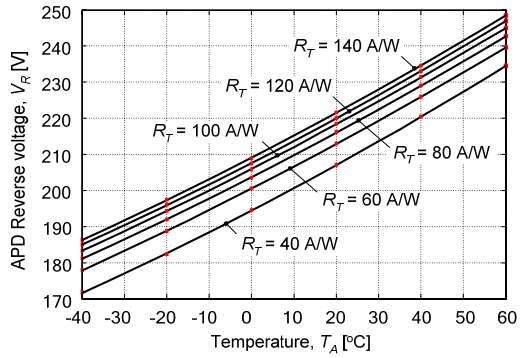

Fig. 10. Reverse voltage in dependence on temperature for constant values of total responsivity.

PWM is controlled by a digital comparator (C). On the assumption that voltage V_C is equal to V'_D it holds for the output voltage

$$V_R = V_C\left(1 + R_1/R_2\right). \tag{22}$$

Substituting (22) into (21) it is obvious that the microcontroller has to calculate the voltage

$$V_C = f\left(T_A\right) = \frac{0.92 \cdot 10^{-3} T_A{}^2 + 0.60 T_A + V_R(0)}{1 + R_1/R_2} \tag{23}$$

where the temperature $T_A = f(V_{TA})$ has to be solved for the temperature sensor used as the inverse of a given or measured dependence $V_{TA} = f(T_A)$. The advantage of the use of microcontroller consists in the easy modification of the voltage V_C calculation, when another APD or temperature sensor is used.

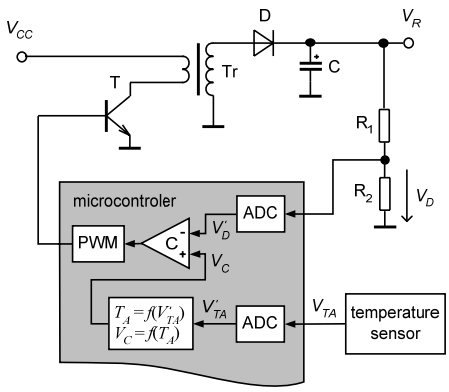

Fig. 11. Connection of switched power supply providing supply voltage for the diode.

7. Conclusion

The results presented above were demonstrated on the connection of a small-area silicon APD operating in the wavelength range from 820 to 1150 nm with a transimpedance preamplifier using a junction transistor. It is obvious that the receiver sensitivity depends on temperature very strongly. The increase in temperature from -40ºC to 60ºC causes the sensitivity degradation by about 6 dB. The sensitivity of another combination of APD and preamplifier can be roughly estimated using the above characteristics. Large-area APDs produce a higher dark current, which increases the sensitivity loss at lower data rates and at higher reverse voltages. Similarly, the multiplied dark current of the InGaAs APDs is usually higher than in the case of silicon APDs, and in combination with the relatively high carrier ionization ratio, which increases the excess noise factor, the InGaAs APDs are evidently noisier than the silicon APDs. Furthermore, due to their lower multiplication factor, the sensitivity of the InGaAs APD-based receiver is lower, but the sensitivity loss caused by temperature change is comparable to that in the receiver with silicon APD.

The temperature influence can be eliminated by cooling the photodiode and the preamplifier. If the maximum multiplication factor is not required, the compensation using a change in the photodiode reverse voltage in dependence on temperature can be applied.

Acknowledgment

This work is supported by the Research Programme MSM0021630513, *Advanced electronic communication systems and technologies* and by the Grant Agency of the Czech Republic project No. 102/06/1358 *Methodology of high-reliability free space optical link design.*

References

[1] ALEXANDER, B. S. *Optical Communication Receiver Design*. SPIE Optical Engineering Press, Washington, 1997.

[2] PERSONICK, S. D. Receiver design for digital fiber optic communication systems, Part I and II. *Bell System Technical Journal*, 1973, vol. 52, no. 6, p. 843–886.

[3] MUOI, T. V. Receiver design for optical-fiber systems. *Journal of Lightwave Technology*, 1984, vol. 2, no. 3, p. 243–265.

[4] Perkin Elmer, *Silicon Avalanche Photodiodes C30902E, C30902S, C30921E, C30921S*. Optoelectronics product data sheet, [online] <http://optoelectronics.perkinelmer.com>.

[5] Perkin Elmer, *High-Performance Emitters & Detectors for the Most Demanding Applications.* [online] <http://optoelectronics. perkinelmer.com>.

[6] PROKES, A., ZEMAN, V. Temperature compensation of the responsivity of avalanche photodiodes in free-space optical communication systems. In *Proc. IEEE-Siberian Conference on Control and Communications SIBCON-2003*. Tomsk (Russia), 2003, p. 102–107.

About Author

Aleš PROKEŠ was born in Znojmo in 1963. He received the M.S. and the Ph.D. degree from the Brno University of Technology in 1988 and 2000, respectively. He is currently working as assistant professor at the Department of Radio Electronic, Brno University of Technology. His research interest includes signal processing and free space optical communication.